Lattice location of Pr^{3+} ions in $LiNbO_3$

A. Lorenzo,* H. Jaffrezic, and B. Roux
Groupe de Traitements de Surfaces, Institut de Physique Nucleaire, Université Claude Bernard Lyon I, 69622 Villeurbanne cedex, France

G. Boulon
Laboratoire de Physico-Chimie de Materiaux Luminescents, Université Claude Bernard Lyon I, Bât. 205, 69622 Villeurbanne cedex, France

L. E. Bausá and J. García-Solé
Departamento de Física de Materiales, Universidad Autónoma de Madrid, Cantoblanco, 28049 Madrid, Spain
(Received 4 April 1995)

Site-selective spectroscopy and Rutherford backscattering spectrometry/channelling techniques are combined to carry out a systematic investigation of the local structure of the different Pr^{3+} centers formed in $LiNbO_3$. Channeling experiments reveal that Pr^{3+} ions are located in Li^+ octahedral sites, but off-center from the regular Li^+ position towards the nearest oxygen plane by about 0.4 Å. Site-selective spectroscopy experiments detect the presence of at least four non-equivalent Pr^{3+} centers. The spectroscopic properties of these centers are also analyzed and explained as a result of the previously mentioned displacements.

I. INTRODUCTION

In the last decades the study of the physical properties of lithium niobate ($LiNbO_3$) has become of great interest. Its excellent electro-optic and acousto-optic properties have permitted the development of a variety of devices which, together with the important applications derived from its photorefractive effect, fully justify the huge effort performed in the investigation of this material. Coherent stimulated emission was demonstrated in rare-earth-activated $LiNbO_3$ by Johnson and Ballman in 1969,[1] and some important features such as self-frequency doubling and self-Q-switching operations have also been obtained in $LiNbO_3$:MgO:Nd,[2,3] opening a new class of interesting devices mainly in optoelectronics. The preparation of $LiNbO_3$ waveguides allows the utilization of this material in integrated optics and minilasers.[4]

A key problem in these rare-earth-doped systems has been to determine the lattice location of the impurity. This is of importance because some of their attractive features depend on the crystal field surrounding the dopant ion, i.e., the site location. Optical spectroscopy (absorption and fluorescence) is very sensitive to changes in local environments and much work in site-selective spectroscopy (SSS) has been performed to understand the multicenter structure in doped $LiNbO_3$.[5–7] Nevertheless, a definitive assignment cannot be done with only optical information. Other techniques such as electron paramagnetic resonance (EPR) have also been applied to some rare-earth-doped $LiNbO_3$ in an attempt to solve the problem of their lattice location. However, the spectra were too broad to obtain a reliable conclusion.[8,9]
On the other hand, an old method, such as ion-beam channeling, was applied a few years ago to the complicated structure of $LiNbO_3$ for the location of impurities. This method, which has been widely used in cubic systems,[10] has become a very powerful tool in the study of rare-earth-doped $LiNbO_3$. Initially, Rutherford backscattering spectroscopy (RBS) experiments were interpreted in terms of a double occupancy (Li^+ and Nb^{5+}) for some rare earths such as Eu^{3+} and Nd^{3+}.[11,12] This led us to discuss the problem of multicenters assuming the occupation of these two sites.[13,14] However, a later comprehensive work by of Rebouta *et al.* using computer simulations provided a definitive interpretation that ruled out the double occupancy for the previously mentioned ions.[15] In addition, a complete catalog to locate impurity ions in this matrix and even to estimate displacements from regular lattice sites was given.

In this paper we have made use of both techniques, laser spectroscopy (LS) together with Rutherford backscattering spectrometry (RBS) channeling experiments, to explain the location of Pr^{3+} ions in $LiNbO_3$ as well as the number and structure of nonequivalent Pr^{3+} centers.

II. EXPERIMENT

Crystals of $LiNbO_3$ with a congruent composition ([Li]/[Nb]=0.945) were grown in our laboratory by the Czochralski method with concentrations of 0.2 and 0.5 mol % of Pr^{3+} in the melt. Samples were oriented using x-ray patterns and carefully polished with alumina powder down to 0.1 μm.

RBS experiments were performed with a 2 MeV Van

der Graaf accelerator in the Institut de Physique Nucleaire de Lyon using a He^+ beam of 1.6 MeV. The samples were mounted on three motors which allowed two rotations and a horizontal displacement. To detect the scattered particles a Si-barrier detector was placed at 172° from the incident beam. Typical currents of 3 nA were used. For SSS, a N_2-pumped dye laser was used as the excitation source, cooling down the samples to 15 K in a closed-cycle He cryostat.

III. EXPERIMENTAL RESULTS

A. RBS channeling

The main signal in a typical RBS spectrum of $LiNbO_3$:Pr^{3+} comes from the particles scattered by Nb^{5+} ions which are the heaviest ones in the matrix. Thus, the lighter elements, Li^+ and O^{2-} ions, are masked by Nb^{5+} ions and cannot be detected. However, this technique is especially sensitive to the rare earth ions which can be detected at higher energies than those corresponding to Nb. These features are shown in Fig. 1, where the Pr^{3+} signal is detected at the high-energy side of the spectrum (see inset). In this figure the channeling effect can also be seen. When the sample is randomly aligned ("random" configuration) the number of scattering Nb^{5+} ions is large and the yield is high. But if we turn the crystal and make one crystallographic axis coincide with the incident particle beam, then the number of scattering ions decreases and so does the particle yield. Only a peak at high energies is observed and attributed to the Nb^{5+} ions in the surface of the crystal.

When the crystal is in a perfectly aligned position the number of scattered particles is very small. Then, if we rotate the sample and depart from this position, the yield increases until we get the random level, which remains constant and is used as the normalization value. These angular scans give us the information to locate the dopant ions inside the crystal.

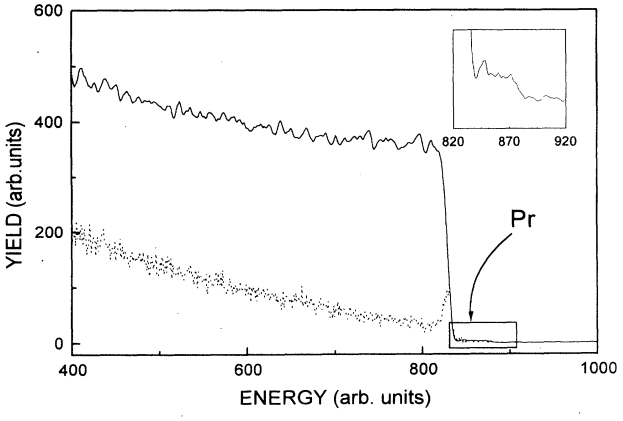

FIG. 1. RBS spectra of Pr^{3+}-doped $LiNbO_3$ for a random orientation of the crystal (solid line) and for the crystal oriented along the $\langle 01\bar{1}0\rangle$ axis (dotted line). The signal corresponding to Pr^{3+} ions is marked with a square at high energies, and enlarged in the inset.

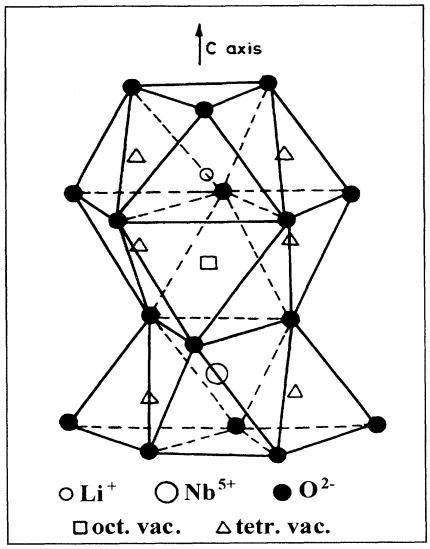

FIG. 2. Part of the unit cell of $LiNbO_3$, showing the four available sites for impurity ions: Li, Nb, octahedral vacancy, and tetrahedral vacancy.

At this point we must take into account the structure of $LiNbO_3$. In Fig. 2 a portion of the unit cell of $LiNbO_3$ is shown, revealing the C_3 (trigonal) point symmetry which describes the crystal. Four possible lattice sites can be conceived for impurity ions: one interstitial site having tetrahedral symmetry, another one with an octahedral environment, and two substitutional sites (Li^+ site and Nb^{5+} site) also with distorted octahedral symmetry. Several directions have been selected as representative to perform the angular variations corresponding to the $\langle 0001\rangle$, $\langle 04\bar{4}5\rangle$, $\langle 02\bar{2}1\rangle$, $\langle 01\bar{1}0\rangle$, and $\langle 11\bar{2}0\rangle$ axes and the (0001) plane. The projections of the lattice structure along these axes are shown in Fig. 3. These projections are very useful to interpret the resulting angular scans and to see whether a Pr^{3+} impurity ion is shielded by the lattice ions or it is in a mid channel position. Here we must note that the multielement nature of $LiNbO_3$ makes quite complicated the analysis of channeling results. However, it is important to emphasize

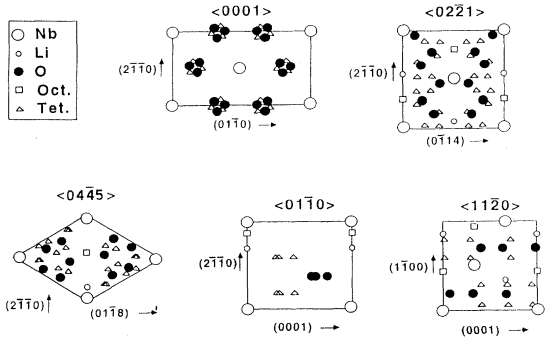

FIG. 3. Projections of the structure of $LiNbO_3$ along some crystallographic directions. The corresponding planes are indicated with arrows.

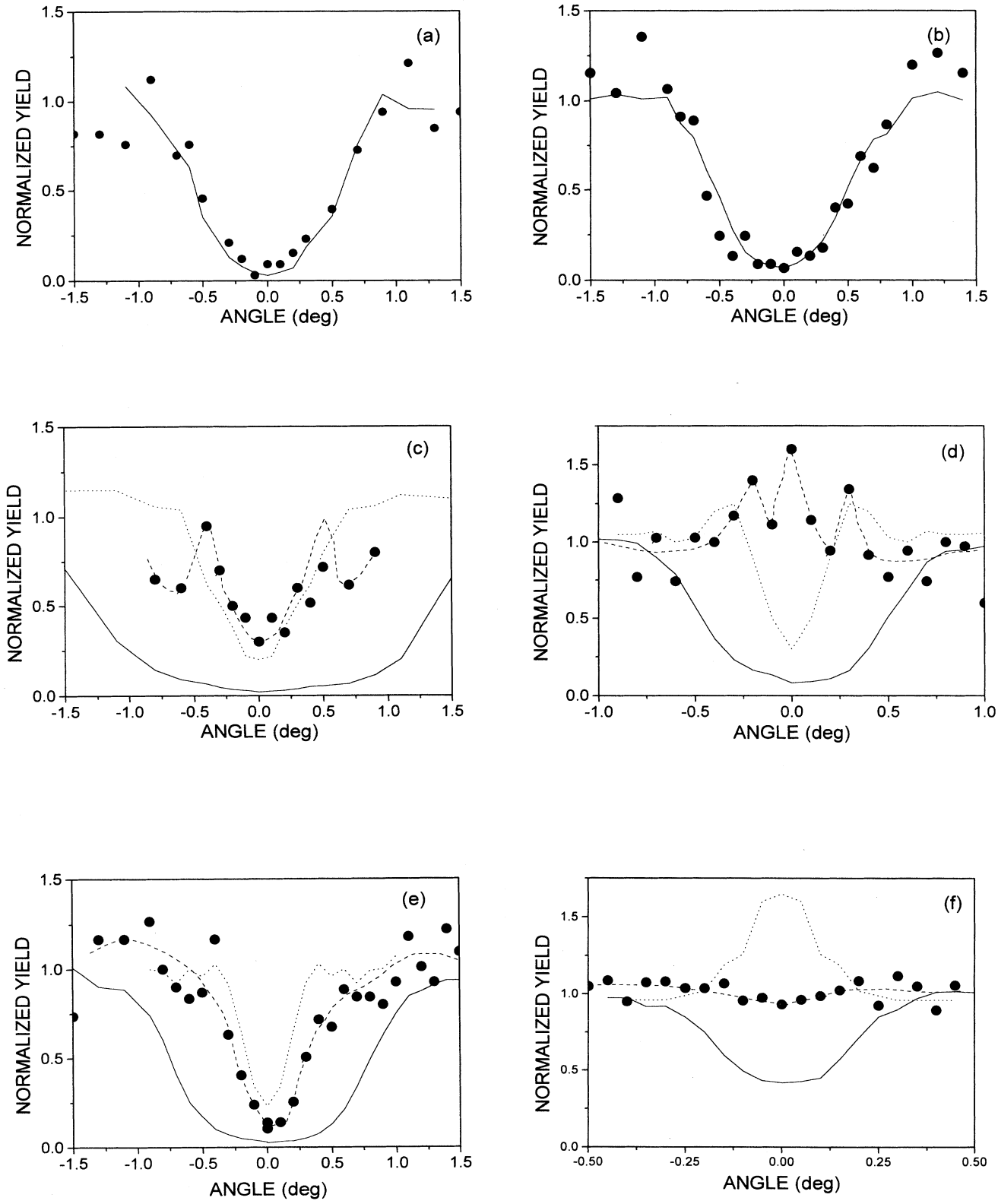

FIG. 4. Angular scans for some representative directions and plane: (a) $\langle 0001 \rangle$, (b) $\langle 04\bar{4}5 \rangle$, (c) $\langle 02\bar{2}1 \rangle$, (d) $\langle 01\bar{1}0 \rangle$, (e) $\langle 11\bar{2}0 \rangle$, and (f) (0001). In all cases the solid line indicates the Nb signal and the solid circles the Pr signal (sometimes a dashed line is drawn as a guide for the eye). In (c) – (f), the dotted line corresponds to the computer simulation for a Li regular position.

that the "channels" for the incident particles will be defined mainly by the Nb^{5+} atomic rows. The Li^+ ions do not contribute to the channeling effect due to their small atomic number as happens with O^{2-} ions. Anyway, the effect of O^{2-} ions can be important in some particular cases, as will be discussed later.

The angular scans obtained for the previously mentioned directions are shown in Figs. 4(a) – 4(f) where the solid line corresponds to the Nb^{5+} signal and the black circles to the Pr^{3+} yield. In some of the scans [Figs. 4(c) –4(f)], the simulated angular variation for ions located in the Li^+ regular position, taken from Rebouta *et al.*,[15] has also been included (dotted line) to be compared with experimental results. These simulated scans for Li^+ ions have been experimentally confirmed by proton-induced x-ray emission (PIXE).[16] For the axial scans a theoretical relation between the half-width of the Nb^{5+} signal, $\psi_{1/2}$, and the Nb^{5+}-Nb^{5+} distance, d, along the axis is found to be proportional to the inverse square root of d.[17] This has been experimentally checked for all our scans, supporting the assignment of axes, which is not an easy task in the complicated structure of $LiNbO_3$.

For the $\langle 0001 \rangle$ channel [Fig. 4(a)] the shape of the dips for Nb^{5+} and Pr^{3+} ions is similar, which indicates that the impurity ions are shielded by the matrix ions and, consequently, they occupy one of the three available octahedral sites along the c axis. A Pr^{3+} ion in an interstitial tetrahedral site would block the channel (see Fig. 3) and the angular scans for Nb^{5+} and Pr^{3+} would be different. Thus, tetrahedral sites must be disregarded for Pr^{3+} ions. The same can be applied to the $\langle 04\bar{4}5 \rangle$ direction [Fig. 4(b)], which has the octahedral vacancy in a mid channel position whereas the angular scans for Nb^{5+} and Pr^{3+} are, again, identical. This allows us to discard the octahedral vacancy site for Pr^{3+} ions. The $\langle 02\bar{2}1 \rangle$ direction [Fig. 4(c)] is used to distinguish between Nb or Li sites because, as can be seen in the corresponding projection, both positions are well separated and, thus, the angular scans should be quite different. In Fig. 4(c) it can be seen that the experimental data for Pr ions are different from the Nb signal and also slightly different from the computer simulation corresponding to a regular Li position [dotted line in Fig. 4(c)], indicating that the impurity is not substituting for Nb^{5+} ions. Thus, Pr^{3+} ions have to occupy the Li^+ octahedron. The difference with the Li position simulation suggests that Pr^{3+} ions substitute for Li^+ ions but are shifted from the Li^+ regular sites along the c axis as has been reported for other rare earth ions in $LiNbO_3$.[15,19] The same result has also been reported for Er^{3+}-doped $LiNbO_3$ by Gog *et al.* using an x-ray standing wave technique.[18] This has to be confirmed with the aid of other significant channels.

In Fig. 3 it can be seen that the axes $\langle 01\bar{1}0 \rangle$ and $\langle 11\bar{2}0 \rangle$ may give us valuable information about the possible displacements from the Li^+ regular site, because the channels are very broad and lithium ions are well separated from niobium and oxygen ions. Moreover, the planar scan (0001) is also very sensitive to the Li^+ position. In all of these figures the simulated-PIXE angular scans for the Li^+ regular ions are also shown to confirm that the Pr^{3+} ions occupy positions different from the regular Li^+ one.

The angular scan along the $\langle 01\bar{1}0 \rangle$ direction [Fig. 4(d)] clearly shows that Pr^{3+} ions occupy a mid channel position which is responsible for the flux peak observed. Computer simulations confirm that the dip corresponding to the regular Li^+ position becomes a flux peak when it is shifted around 0.45 Å along the c axis towards the nearest oxygen plane (negative shift). A similar result can be obtained for the $\langle 11\bar{2}0 \rangle$ axis [Fig. 4(e)] and allows us to predict a negative displacement of the Pr^{3+} ion inside the Li octahedron.

For the planar scan (0001) in Fig. 4(f), the presence of oxygen ions plays an important role in the channeling effect (see also the $\langle 11\bar{2}0 \rangle$ projection in Fig. 3). In fact the larger amounts of these ions relative to Nb^{5+} ions make both electrostatic potentials (O^{2-} and Nb^{5+}) comparable for the incident particles.[20] Thus, the middle of the planar channel is no longer defined by the Nb^{5+} ions but by the Nb^{5+} and oxygen planes. The resulting angular scan for Pr^{3+} ions is again in agreement with a negative shift of around 0.45 Å as can be seen when comparing with the computer simulations.

It must be pointed out that the estimated shift of −0.45 Å should not be considered as an exact position for all the impurity ions. In fact we never obtained an angular scan which fitted perfectly with the computer simulations. It seems more reasonable to think of a distribution of Pr^{3+} ions with shifts from about −0.35 to −0.45 Å (the minus sign indicating a displacement towards the nearest oxygen plane). This is more evident in the scan along $\langle 01\bar{1}0 \rangle$ [see Fig. 4(d)], due to the peaks appearing at both sides of the central flux peak. The central flux peak indicates a mid channel position, while the other peaks suggest positions slightly away from the middle of the channel. As a summary, the contribution of the channeling technique is to determine that the Pr^{3+} ions are located inside the Li^+ octahedra in positions shifted around −0.4 Å along the c axis with respect to the Li^+ regular position.

B. Site-selective spectroscopy

It is customary in the spectroscopy of many rare-earth-doped $LiNbO_3$ systems to find a number of spectral lines greater than those expected by the splitting of Russel-Saunders multiplets in the presence of a crystal field with a particular symmetry.[5,21] These extra lines have been attributed to the existence of impurity ions with different environments (multicenters). This is also observed very clearly in Pr^{3+}-doped $LiNbO_3$, especially in the $^3P_0$ singlet which exhibits a fourfold structure, as can be seen in the low-temperature σ-polarized absorption spectrum ($^3H_4 \rightarrow {}^3P_0$) of Fig. 5.

Selective excitation in each of the four absorption bands, marked by arrows in Fig. 5, will confirm that the observed structure is due to multicenters. Excitation in

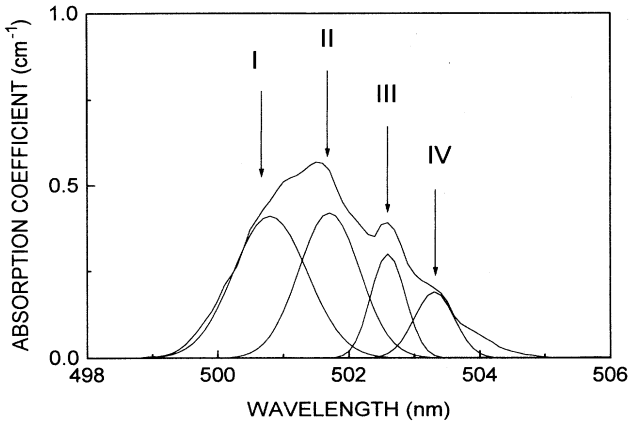

FIG. 5. Absorption spectrum of $LiNbO_3$:Pr^{3+} (0.2 mol %) corresponding to the transition $^3H_4 \rightarrow {}^3P_0$ in σ polarization at 15 K. The structure is fitted to four Gaussian functions and the peaks are indicated by arrows.

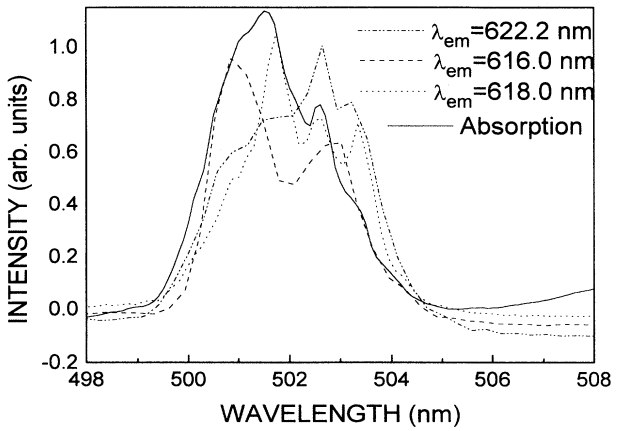

FIG. 7. Excitation spectra of $LiNbO_3$:Pr^{3+} (0.5 mol %) at 15 K for different emission wavelengths of the $^1D_2 \rightarrow {}^3H_4$ transition: dash-dotted line, λ_{em}=622.2 nm; dashed line, λ_{em}=616.0 nm; and dotted line, λ_{em}=618.0 nm. For comparison the absorption spectrum at 15 K is also drawn with solid line.

the $^3P_0$ singlet is quickly nonradiatively relaxed to the $^1D_2$ state, from which luminescence occurs.[22] Fluorescence measurements in this work have been performed in the 600–650 nm region, corresponding to the $^1D_2 \rightarrow {}^3H_4$ transition which is the main emission of Pr^{3+} ions in $LiNbO_3$.[22,23] Figure 6 shows the results of site-selective excitation in the $^3P_0$ state for the 0.2-mol % doped sample, although the same spectra were obtained for the 0.5-mol %-doped one. As can be seen, the fluorescence spectra are different depending on the excitation wavelength, confirming the existence of Pr^{3+} ions with, at least, four different crystal environments (multicenters).

Due to the strong overlapping in the four absorption bands of the $^3H_4 \rightarrow {}^3P_0$ transition, it was difficult to select only one center individually and, thus, the emission spectra always show the contributions of more than one center. The identification of the Stark levels of the $^3H_4$ state corresponding to each center can be performed, however, considering the changes in the relative intensities of the emission lines. Excitation spectra were also useful to confirm the assignment of the Stark levels, especially in the region from 615 to 625 nm where some lines of different centers coincide. Figure 7 shows the $^3H_4 \rightarrow {}^3P_0$ excitation spectra monitoring emission wavelengths contained in the mentioned spectral range, and are also compared with the $^3H_4 \rightarrow {}^3P_0$ absorption spectrum. It can be seen that for each emission wavelength, one of the four overlapping

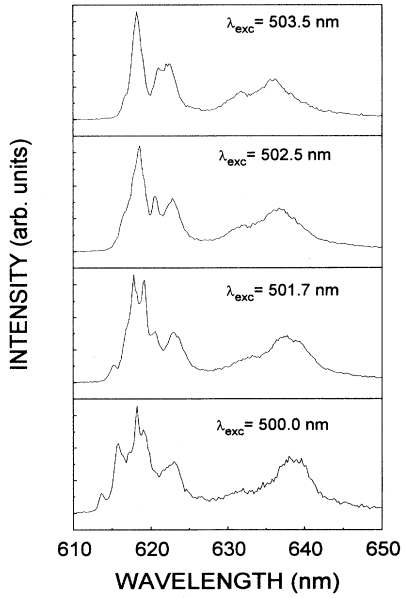

FIG. 6. Fluorescence spectra of Pr^{3+} ion in $LiNbO_3$ in the region of the $^1D_2 \rightarrow {}^3H_4$ transition at 15 K for different excitation wavelengths.

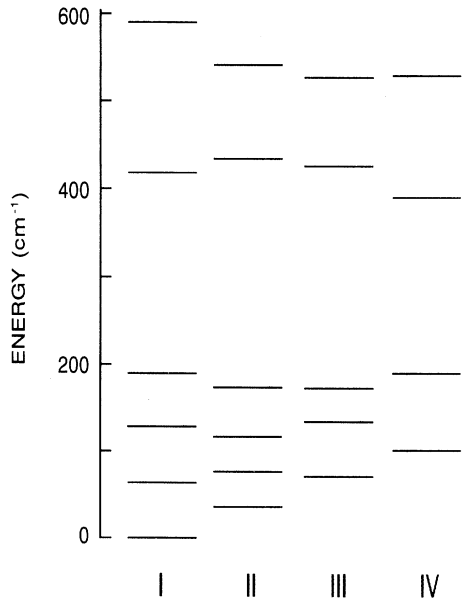

FIG. 8. Energy level diagram of the $^3H_4$ multiplet for each of the four sites labeled I – IV.

absorption bands is promoted, and this permitted the assignment of the Stark levels of the $^3H_4$ multiplet for each center.

With this information we have constructed the energy levels structure of the $^3H_4$ ground state for each center. For doing so, the energy position of the $^3P_0$ singlet has been arbitrarily taken as a constant equal to 19 968 cm^{-1}. The result has been displayed in Fig. 8, and it can be seen that there are important differences in the energy levels structure of this multiplet for each Pr^{3+} center. The first one concerns the total amount of splitting of the multiplet which can be observed that decreases from 585 cm^{-1} (center I) to 420 cm^{-1} (center IV). This fact reveals that the intensity of the crystal field acting on the Pr^{3+} ion is different for each center, being the highest for the one with the highest splitting.

Another important feature emerges from the different number of Stark levels that can be seen in the $^3H_4$ multiplet. It is observed that the six levels appearing in center I become five for center III and four in the case of center IV, which indicates again different crystal environments around the Pr^{3+} ions.

IV. DISCUSSION

Site-selective spectroscopy itself can give us information about the existence and number of nonequivalent centers and eventually their crystal symmetry. However, it is worthwhile to combine it with RBS experiments in order to obtain a better idea about the location of impurity ions.

The first result concluded by RBS is the location of Pr^{3+} ions inside only one kind of octahedron, the Li^+ octahedron, and shifted from the Li^+ regular site along the c axis (off centered). According to this, the different centers detected by SSS can be thought as Pr^{3+} ions in different axial positions inside the Li^+ octahedron.

Once we assume that the ions are located in the same kind of octahedron, the next step is to explain the multicenter structure observed in the optical spectra. From these spectra (absorption and fluorescence) it can be noticed that the difference between the centers is much larger than the inhomogeneous broadening due to strains in the lattice. Thus, we can assume that the different crystal environments consist of perturbations of the octahedral arrangement. This means that, if we consider that the oxygen ions keep their place, the Pr^{3+} ion position should change from center to center. Of course, care must be taken with the assumption of a fixed oxygen environment, but the possible oxygen displacements in the vicinity of Pr^{3+} ions cannot be determined either by RBS or by SSS experiments.

On the other hand, the results of RBS experiments also prove that any Pr^{3+} position should be along the c axis, because no Pr^{3+} ions were detected away from this axis. Consequently, the four centers could correspond to different displacements from the regular Li^+ site along the c axis. This is supported by the optical data concerning the $^3H_4$ splitting for each center. In addition, a similar center structure has been proposed for Nd^{3+} ions in $LiNbO^{3+}$.[19] In the case of Pr^{3+} ions, it can be seen that the Stark splitting decreases from center I to center IV, indicating a decreasing crystal field intensity on the ion position.

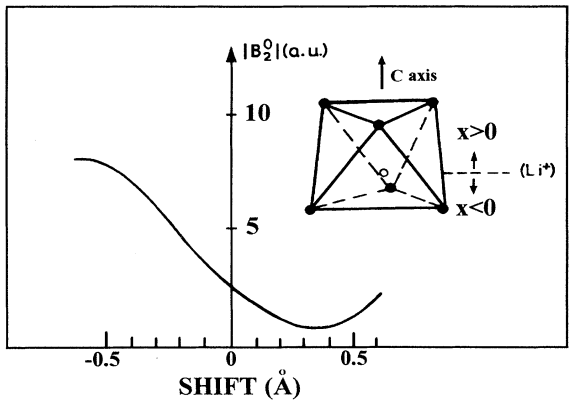

FIG. 9. Variation of the crystal field parameter B_0^2 (in arb. units) as a function of the displacement from the regular Li^+ site along the c axis.

The shift along the c axis is mainly responsible for the trigonal distortion to the octahedral symmetry of the impurity ions in the $LiNbO_3$ octahedra. This axial distortion is controlled by the crystal field parameter B_2^0, which can be calculated using a point charge environment approximation as in Faucher and Caro.[24] The result is displayed in Fig. 9, where this parameter is plotted as a function of the displacement along the c axis. This dependence shows that the more off-centered the impurity is located, the less cubic the crystal environment is. In fact, this could explain the change in the number of Stark levels observed in Fig. 8, which is equal to six in trigonal symmetry and to four in cubic symmetry.[25] Hence, the center labeled I should be the most off centered while the one labeled IV should be the most centered.

However, according to RBS measurements, all Pr^{3+} ions are located in a region around 0.4 Å from the regular Li^+ site towards the nearest oxygen plane, which indicates that different optical centers should be contained in that range.

The reason for these different off-centered positions has to be related to the lattice defects associated with the nonstoichiometry of the matrix. The Li^+ deficiency is compensated with the creation of defects such as Nb^{5+} antisites (Nb^{5+} ions in a Li^+ site) and Nb^{5+} vacancies.[26] These defects could come to the proximity of Pr^{3+} ions to compensate the 2+ net charge produced when substituting for Li^+ ions and thus the local environment of the impurity can be modified giving place to nonequivalent centers.[27] In any case, at the present time, a model is lacking to explain the charge compensation mechanisms for rare earths in $LiNbO_3$.

V. CONCLUSION

In this paper we have made use of two different techniques (optical spectroscopy and RBS channeling) to lo-

cate the Pr^{3+} ions in $LiNbO_3$. Both techniques have proved to be complementary in the information about the number and position of different Pr^{3+} centers. RBS-channeling experiments for a number of crystallographic directions have permitted the localization of the impurity ions in the $LiNbO_3$ host lattice. Axial and planar scans have shown that the Pr^{3+} ions are located in the Li^+ octahedra, but shifted from the regular Li^+ site towards the nearest oxygen plane. The amount of the displacement has been estimated to be around 0.4 Å.

On the other hand, site-selective spectroscopy has proved the presence of at least four nonequivalent centers, labeled I, II, III, and IV. A simplified energy level diagram has been constructed for the $^3H_4$ ground state of each Pr^{3+} center.

The combination of both techniques permitted us to establish how the Pr^{3+} ions are distributed and located in $LiNbO_3$. This impurity is incorporated substituting for Li^+ ions and occupies a position shifted from the regular Li^+ site. The different optical centers can be identified as Pr^{3+} ions occupying slightly different positions inside the Li^+ octahedron in the region from 0.35 to 0.45 Å from the regular Li^+ site towards the nearest oxygen plane.

ACKNOWLEDGMENTS

This paper has been supported by the Comisión Interministerial de Ciencia y Tecnología (CICYT) under Project No. MAT 95-0152. The authors wish to acknowledge Dr. J. A. Sanz-García and J. E. Muñoz-Santiuste for fruitful discussions.

* Present address: Departamento de Física de Materiales, Universidad Autónoma de Madrid, Cantoblanco, 28049 Madrid, Spain.

[1] F. Johnson and A. A. Ballman, J. Appl. Phys. **40,** 297 (1969).
[2] E. Lallier, J. P. Pocholle, M. Papuchon, M. de Micheli, J. M. Li, Q. He, D. B. Ostrowski, C. Grezes-Besset, and E. Pelletier, Opt. Lett. **15,** 682 (1990).
[3] A. Córdova-Plaza, M. Digonnet, and H. J. Shaw, IEEE J. Quantum Electron. **QE-23,** 262 (1987).
[4] S. J. Field, D. C. Hanna, D. P. Shepherd, A. C. Tropper, P. J. Chandler, P. D. Townsend, and L. Zhang, Opt. Lett. **16,** 481 (1991).
[5] A. Lorenzo, L. E. Bausá, and J. García Solé, J. Phys. Condens. Matter **6,** 1065 (1994).
[6] R. Duchowicz, L. Núñez, J. O. Tocho, and F. Cussó, Solid State Commun. **88,** 439 (1993).
[7] D. M. Gill, J. C. Wright, and L. McCaughan, Appl. Phys. Lett. **64,** 2483 (1994).
[8] G. Burns, D. F. O'Kane, and R. S. Title, Phys. Rev. **167,** 314 (1968).
[9] D. M. B. P. Milton, I. J. Moraes, A. C. Hernandes, R. R. De Souza, M. Siu Li, M. C. Terrile, and G. E. Barberis, Phys. Rev. B **51,** 3206 (1995).
[10] T. Picraux, in *New Uses of Ion Accelerators*, edited by S. F. Ziegler (Plenum, New York, 1975).
[11] L. Rebouta, J. C. Soares, M. F. da Silva, J. A. Sanz García, E Diéguez, and F. Agulló-López, Appl. Phys. Lett. **55,** 120 (1989).
[12] L. Rebouta, J. C. Soares, M. F. da Silva, J. A. Sanz García, E. Diéguez, and F. Agulló-López, J. Mater. Res. **7,** 1 (1992).
[13] G. Lifante, F. Cussó, F. Jaque, J. A. Sanz García, A. Monteil, B. Varrel, G. Boulon, and J. García Solé, Chem. Phys. Lett. **176,** 482 (1991).
[14] J. E. Muñoz Santiuste, B. Macalik, and J. García Solé, Phys. Rev. B **47,** 88 (1993).
[15] L. Rebouta, P. J. M. Smulders, D. O. Boerma, F. Agulló-López, M. F. da Silva, and J. C. Soares, Phys. Rev. B **48,** 3600 (1993).
[16] L. Kovacs, L. Rebouta, J. C. Soares, and M. F. Da Silva, Radiat. Eff. Defects Solids **119-121,** 445 (1991).
[17] *Channeling*, edited by D. V. Morgan (John Wiley & Sons, London, 1973).
[18] T. Gog, M. Griebenow, and G. Materlik, Phys. Lett. A **181,** 417 (1993).
[19] J. García Solé, T. Petit, H. Jaffrezic, and G. Boulon, Europhys. Lett. **24,** 719 (1993).
[20] L. Rebouta, M. F. da Silva, J. C. Soares, M. Hage-Ali, J. P. Stoquert, P. Siffert, J. A. Sanz-García, E. Diéguez, and F. Agulló-López, Europhys. Lett. **14,** 557 (1991).
[21] L. Núñez and F. Cussó, J. Phys. Condens. Matter **5,** 5301 (1993).
[22] A. Lorenzo, L. E. Bausá, and J. García Solé, Phys. Rev. B **51,** 16 643 (1995).
[23] A. Lorenzo, L. E. Bausá, M. Voda, and J. García Solé, J Phys. (France) Colloq. IV **4,** C4-381 (1994).
[24] M. Faucher and P. Caro, J. Chem. Phys. **63,** 446 (1975).
[25] B. Henderson and G. P. Imbusch, *Optical Spectroscopy of Inorganic Solids* (Clarendon, Oxford, 1989).
[26] C. Abrahams and P. Marsh, Acta Crystallogr. B **12,** 61 (1986).
[27] J. García Solé, Phys. Scr. T **55,** 30 (1994).